Interconverting Edge-Sharing and Face-Sharing Bioctahedral Dinuclear Tungsten(III) Complexes. Preparations, Properties, and Structures of $W_2Cl_6L_4$, Where L = PMe_3, PEt_3, and $P(n\text{-}Bu)_3$, $W_2Cl_6L_3$, Where L = PEt_3 and $P(n\text{-}Bu)_3$, and $[HPEt_3]^+[W_2Cl_7(PEt_3)_2]^-$

Jane T. Barry, Stephanie T. Chacon, Malcolm H. Chisholm,* Vince F. DiStasi, John C. Huffman, William E. Streib, and William G. Van Der Sluys

Department of Chemistry and Molecular Structure Center, Indiana University, Bloomington, Indiana 47405

Received October 15, 1992

In tetrahydrofuran solution the sodium salt of the $[W_2Cl_7(THF)_2]^-$ anion and the tertiary phosphines PR_3 (≥4 equiv) react at room temperature to give red crystalline compounds $W_2Cl_6(PR_3)_4$, where R = Me, Et, and *n*-Bu. The compounds where R = Me and Et have been characterized by single-crystal X-ray crystallography and were shown to contain an edge-shared bioctahedral (ESBO) geometry $Cl_2P_2W(\mu\text{-}Cl)_2WCl_2P_2$ with W–W = ca. 2.72 Å. The arrangement of the terminal ligands is such that at one W atom there are cis Cl and trans PR_3 ligands while at the other W atom the order is reversed. Crystal data: for $W_2Cl_6(PMe_3)_4$ at −152 °C, a = 11.049(2) Å, b = 18.004(5) Å, c = 13.667(4) Å, β = 96.29(1)°, Z = 4, d_{calcd} = 2.18 g cm^{-3}, and space group $P2_1/a$; for $W_2Cl_6(PEt_3)_4$ at −141 °C, a = 11.220(2) Å, b = 18.462(3) Å, c = 18.519(3) Å, Z = 4, d_{calcd} = 1.84 g cm^{-3}, and space group $P2_1/n$. In hydrocarbon solutions the ESBO complexes exist in equilibrium with face-shared bioctahedral (FSBO) complexes $W_2Cl_6(PR_3)_3$ and free PR_3, where R = Et and *n*-Bu. Crystal data for $W_2Cl_6(PEt_3)_3\cdot CH_2Cl_2$ at −144 °C: a = 14.097(2) Å, b = 12.992(2) Å, c = 18.798(3) Å, β = 97.96(1)°, Z = 4, d_{calcd} = 1.99 g cm^{-3}, and space group $P2_1/n$. The molecule contains a central FSBO $P_2ClW(\mu\text{-}Cl)_3WCl_2P$ core that has a virtual mirror plane of symmetry and the NMR data obtained are consistent with this isomeric form being present in solution. The W–W distance 2.471(1) Å in the FSBO complex is notably shorter than those in the ESBO complexes. The equilibrium $W_2Cl_6(PEt_3)_4 \rightleftarrows W_2Cl_6(PEt_3)_3 + PEt_3$, has been studied in toluene-d_8 by NMR spectroscopy over the temperature range +22 to −15 °C. From measurements of K_{eq}, the thermodynamic parameters were evaluated: $\Delta H°$ = −2.5 (±0.5) kcal mol^{-1} and $\Delta S°$ = −4 (±2) eu. The formation of the ESBO complex $W_2Cl_6(PEt_3)_4$ from the FSBO complex $W_2Cl_6(PEt_3)_3$ was studied in the presence of an excess of PEt_3 in the temperature range +22 to −10 °C. Under these conditions the reaction showed a first-order dependence on [PEt_3]. The activation parameters, $\Delta H^‡$ = +8 (±1) kcal mol^{-1} and $\Delta S^‡$ = −50 (±8) eu, are consistent with a bimolecular reaction. An impurity often encountered in hydrocarbon solutions of $W_2Cl_6(PEt_3)_n$, where n = 4 or 3, was shown to be $[HPEt_3]^+[W_2Cl_7(PEt_3)_2]^-$. Crystal data at −166 °C: a = 12.011(4) Å, b = 33.54(1) Å, c = 16.685(6) Å, β = 107.73(1)°, Z = 8, d_{calcd} = 2.015 g cm^{-3}, and space group $P2_1/a$. In the solid state there is an enantiomeric pair of *gauche*-$[W_2Cl_7(PEt_3)_2]^-$ anions each weakly associated with the countercation $[HPEt_3]^+$ by hydrogen bonding. The FSBO $PCl_2W(\mu\text{-}Cl)_3WClP_2$ cores and the W–W distances of 2.438(2) and 2.427(2) Å for the two enantiomers are very similar. A preparation of $[HPEt_3]^+[W_2Cl_7(PEt_3)_2]^-$ involved either (i) addition of $[HPEt_3]^+Cl^-$ (1 equiv) to $W_2Cl_6(PEt_3)_4$ in hydrocarbon solutions or (ii) the reaction between $NaW_2Cl_7(THF)_5$, PEt_3 (4 equiv), and H_2O (2 equiv) in tetrahydrofuran. These findings are discussed in terms of the factors influencing the interconversion of d^3–d^3 FSBO and ESBO complexes and are comparerd with the recent studies of Cotton and Mandal [*Inorg. Chem.* **1992**, *31*, 1267].

Introduction

In 1958, Hawkins and Garner[1] studied the chloride ion exchange reaction shown in eq 1 by use of ^{36}Cl and found that all nine

$$W_2Cl_9^{3-} + 9{}^*Cl^- \rightleftarrows W_2{}^*Cl_9^{3-} + 9Cl^- \qquad (1)$$

chlorine atoms of $W_2Cl_9^{3-}$ were "kinetically equivalent in the exchange despite their structural non-equivalence".

Under the conditions required to preserve the $W_2Cl_9^{3-}$ ion in aqueous media it was not possible to investigate the dependence of rate on [Cl^-] and the authors suggested that one of two possibilities could account for the observed Cl^- exchange. (1) An opening and closing of bridges (intramolecular) was occurring with concurrent intermolecular Cl^- exchange, or (2) the exchange was proceeding by way of a dynamic equilibrium involving $W_2Cl_9^{3-}$ and other species such as $W_3Cl_{14}^{5-}$ and WCl_5^{2-}. Hawkins and Garner favored the second of the two alternatives. However, some 10 years later, Hayden and Wentworth[2] reported the facile synthesis of $W_2Br_9^{3-}$ according to the reaction shown in eq 2, and

$$W_2Cl_9^{3-} + \text{excess } Br^- \text{ [in } c\text{HBr(aq)]} \rightarrow W_2Br_9^{3-} + 9Cl^- \qquad (2)$$

on the basis of their studies of the reaction, commented as follows: "In the light of these observations, we can find no present reason to discard the first mechanism discussed by Hawkins and Garner.... The existence of a ten-coordinate dinuclear ion ($W_2Cl_{10}^{4-}$) seems reasonable in view of the recent preparation and structural characterization of $W_2Cl_6(py)_4$."

Recent work in this laboratory showed that reduction of WCl_4 in tetrahydrofuran (THF) by Na/Hg yielded the anion $[W_2Cl_7(THF)_2]^-$, which was crystallographically characterized

(1) Hawkins, G. L.; Garner, C. S. *J. Am. Chem. Soc.* **1958**, *80*, 2946.

(2) Hayden, J. L.; Wentworth, R. A. D. *J. Am. Chem. Soc.* **1968**, *90*, 5291.

0020-1669/93/1332-2322$04.00/0

Table I. Summary of Crystal Data[a]

	I	II	III	IV
empirical formula	$W_2Cl_6P_4C_{12}H_{36}$	$W_2Cl_6P_4C_{24}H_{60}$	$W_2Cl_8P_3C_{19}H_{47}$	$C_{18}H_{46}Cl_7P_3W_2$
cryst dimens, mm	0.12 × 0.15 × 0.25	0.12 × 0.20 × 0.25	0.24 × 0.24 × 0.28	0.04 × 0.26 × 0.26
space group	$P2_1/a$	$P2_1/n$	$P2_1/n$	$P2_1/a$
temp, °C	−152	−141	−144	−166
a, Å	11.049(2)	11.220(2)	14.097(2)	12.011(4)
b, Å	18.004(5)	18.462(3)	12.992(2)	33.54(1)
c, Å	13.667(14)	18.519(3)	18.798(3)	16.685(6)
β, deg	96.29(1)	98.32(1)	97.96(1)	107.73(1)
Z (molecules/cell)	4	4	4	8
V, Å^3	2702.37	3795.79	3409.54	6401.64
calcd density, g/cm^3	2.175	1.843	1.987	2.015
wavelength, Å	0.710 69	0.710 69	0.710 69	0.710 69
mol wt	884.73	1053.05	1019.83	971.35
linear abs coeff, cm^{-1}	95.252	67.964	76.724	80.834
no. of reflns				
with $F > 0.0$		4644	4324	7061
with $F > 3.00\sigma(F)$	2979	4288	4125	4550
$R(F)$[b]	0.0336	0.0397	0.0437	0.0730
$R_w(F)$[c]	0.0342	0.0397	0.0445	0.0715

[a] I = $W_2Cl_6(PMe_3)_4$; II = $W_2Cl_6(PEt_3)_4$; III = $W_2Cl_6(PEt_3)_3{\cdot}CH_2Cl_2$; IV = $(Et_3PH)W_2Cl_7(PEt_3)_2$. [b] $R(F) = \sum(|F_o| - |F_c|)/\sum|F_o|$. [c] $R_w(F) = [\sum w(|F_o| - |F_c|)^2/\sum w|F_o|^2]^{1/2}$.

both as a sodium salt, $NaW_2Cl_7(THF)_5$,[3] and as a phosphonium salt, $(Ph_4P)W_2Cl_7(THF)_2{\cdot}^1/_2CH_2Cl_2$.[4] On the basis of UV–vis spectroscopy in CH_2Cl_2, THF, and the solid state, we were able to show that the face-shared bioctahedral (FSBO) structure was present under all conditions. Specifically, in THF solution we found no evidence for the existence of an equilibrium of the type shown in eq 3.

$$W_2Cl_7(THF)_2^- + 2THF \rightleftarrows W_2Cl_6(THF)_4 + Cl^- \quad (3)$$

In view of the ability of $W_2Cl_9^{3-}$ and $W_2Cl_7(THF)_2^-$ to react with pyridine to give $W_2Cl_6(py)_4$ we became interested in what factors favor the confacial versus the edge-shared bioctahedral (ESBO) geometry. We describe here our discovery of an equilibrium involving the two geometries[5] and offer some general comments concerning factors favoring each geometry. Furthermore, from variable temperature studies of the equilibrium shown in eq 4, we report the thermodynamic parameters for the

$$\underset{\text{ESBO}}{W_2Cl_6(PEt_3)_4} \rightleftarrows \underset{\text{FSBO}}{W_2Cl_6(PEt_3)_3} + PEt_3 \quad (4)$$

interconversion of face- and edge-shared bioctahedra along with an estimation of the activation parameters. These studies provide insight into the intimate mechanism of nucleophilic substitution by a tertiary phosphine on the FSBO complex.

Results and Discussion

Synthesis. Addition of PR_3 (>10 equiv) to solutions of $NaW_2Cl_7(THF)_5$ in tetrahydrofuran leads to an immediate color change from green to red. After removal of the solvent under a dynamic vacuum, the compounds $W_2Cl_6L_4$, where L = PMe_3, PEt_3 and $P(n\text{-}Bu)_3$, were obtained by extraction and crystallization from CH_2Cl_2/hexane or CH_2Cl_2/Et_2O. Similar compounds were not isolated for the more bulky phosphines PPh_3 and $PMePh_2$.

Recently Cotton and Mandal[6] reported a series of ESBO and FSBO complexes of general formula $W_2X_6(PR_3)_n$ where X = Cl or Br, PR_3 = PMe_3, PMe_2Ph, or $P(n\text{-}Bu)_3$, and n = 3 or 4 together with the X-ray structural characterization of $W_2Cl_6(PMe_2Ph)_n$, where n = 3 and 4, and $W_2Br_6(PMe_2Ph)_3$. The preparative procedure adopted by Cotton and Mandal[6] involved one-pot syntheses starting from WCl_4 and 1 equiv of the reducing agent, Na/Hg or $NaHBEt_3$, in toluene followed by direct addition of the appropriate tertiary phosphine (n equiv). Synthetically this procedure is simpler than ours which involves the preparation and isolation of the intermediate $[W_2Cl_7(THF)_2]^-$ salt. However, our reaction is mechanistically more elementary and focuses on the need to understand the nature of the interconversion of the FSBO and ESBO complexes.

During the course of our studies we discovered a commonly occurring impurity which, frustratingly, when present impeded the study of the equilibrium (4). The impurity was shown to be $[HPEt_3]^+[W_2Cl_7(PEt_3)_2]^-$, which is readily formed upon the addition of H_2O to the species present in eq 4. Indeed, the phosphonium salt can be prepared in 70% isolated crystalline yield based on W according to the reaction shown in eq 5. (No

$$NaW_2Cl_7(THF)_5 + 3PEt_3 + 3H_2O \rightarrow [HPEt]^+[W_2Cl_7(PEt_3)_2]^- \quad (5)$$

knowledge of stoichiometry is available.) We have traced the fate of the oxygen atoms in reaction 5 to the formation of the tetranuclear cluster $[W_4(\mu\text{-}O)_3Cl_7(PEt_3)_3]^-$, which can also be isolated as a $[HPEt_3]^+$ salt. (The structure and bonding in this unusual 12-electron tetrahedral tungsten cluster will be described elsewhere.[7]) A direct synthesis of the salt $[HPEt_3]^+[W_2Cl_7(PEt_3)_2]^-$ that does not involve adventitious water was found to involve the addition of $[HPEt_3]^+Cl^-$ to $W_2Cl_6(PEt_3)_4$ in toluene, eq 6.

$$W_2Cl_6(PEt_3)_4 + [HPEt_3]^+Cl^- \rightarrow [HPEt_3]^+[W_2Cl_7(PEt_3)_2]^- + 2PEt_3 \quad (6)$$

In hydrocarbon solvents the Cl^- anion converts the species present in the ESBO ⇄ FSBO equilibrium (eq 4) to the FSBO $[W_2Cl_7(PEt_3)_2]^-$ anion with liberation of free PEt_3. By ^{31}P NMR spectroscopy there is evidently exchange between $[HPEt_3]^+$ and PEt_3 by proton transfer which leads to line-broadening and impedes the observation of eq 4. The rigorous use of anhydrous solvents and flamed/vacuum-dried glassware did allow the

(3) (a) Chisholm, M. H.; Eichhorn, B. W.; Folting, K.; Huffman, J. C.; Ontiveros, C. D.; Streib, W. E.; Van Der Sluys, W. G. *Inorg. Chem.* **1987**, *26*, 3182. (b) The formulation for this compound was originally suggested to be $W_2Cl_6(THF)_4$: Sharp, P. R.; Schrock, R. R. *J. Am. Chem. Soc.* **1980**, *102*, 1430.

(4) Bergs, D. J.; Chisholm, M. H.; Folting, K.; Huffman, J. C.; Stahl, K. A. *Inorg. Chem.* **1988**, *27*, 2950.

(5) Chacon, S. T.; Chisholm, M. H.; Streib, W. E.; Van Der Sluys, W. G. *Inorg. Chem.* **1989**, *28*, 5.

(6) Cotton, F. A.; Mandal, S. K. *Inorg. Chem.* **1992**, *31*, 1267.

(7) Barry, J. T.; Chacon, S. T.; Chisholm, M. H.; Folting, K.; Martin, J. C. *J. Cluster Sci.*, in press.

Table II. Fractional Coordinates and Isotropic Thermal Parameters for $W_2Cl_6(PMe_3)_4$

atom	10^4x	10^4y	10^4z	$10B_{iso}$, Å^2
W(1)	8904.7(3)	598.6(2)	2519.3(3)	11
W(2)	7322.0(3)	-552.6(2)	2515.3(3)	12
Cl(3)	7787(2)	108(1)	1069(2)	15
Cl(4)	8486(2)	-50(1)	3955(2)	16
Cl(5)	10298(2)	1277(1)	3742(2)	18
Cl(6)	9593(2)	1457(1)	1298(2)	19
Cl(7)	5434(2)	110(1)	2582(2)	19
Cl(8)	8694(2)	-1587(1)	2422(2)	21
P(9)	7458(2)	1649(1)	2785(2)	15
P(10)	10808(2)	-129(1)	2292(2)	16
P(11)	6418(2)	-1281(1)	3866(2)	16
P(12)	6127(2)	-1347(2)	1166(2)	18
C(13)	12139(10)	471(7)	2217(9)	27
C(14)	10799(10)	-678(6)	1173(8)	21
C(15)	11356(10)	-746(6)	3306(8)	22
C(16)	8198(10)	2551(6)	2958(8)	22
C(17)	6655(10)	1601(6)	3873(8)	22
C(18)	6314(10)	1834(6)	1772(8)	24
C(19)	4817(11)	-1540(7)	3634(9)	30
C(20)	6405(10)	-789(6)	5022(8)	23
C(21)	7159(12)	-2148(6)	4232(9)	30
C(22)	6720(11)	-1349(7)	-1(9)	29
C(23)	6065(11)	-2347(6)	1406(9)	29
C(24)	4522(10)	-1136(7)	857(9)	33

observation of eq 4 with imperceptible amounts of the compound $[HPEt_3]^+[W_2Cl_7(PEt_3)_2]^-$.

Structural Studies: $W_2Cl_6L_4$ (L = PMe_3 and PEt_3), $W_2Cl_6(PEt_3)_3$, and $[HPEt_3]^+[W_2Cl_7(PEt_3)_2]^-$. A summary of crystal data is given in Table I, and fractional coordinates for the four structurally characterized compounds are given in Tables II–V. ORTEP drawings are given in Figures 1–4, and pertinent bond distances and angles for $W_2Cl_6(PMe_3)_4$ and $W_2Cl_6(PEt_3)_4$ are given in Table VI and those for $W_2Cl_6(PEt_3)_3$ and $[HPEt_3]^+[W_2Cl_7(PEt_3)]^-$ are given in Tables VII and VIII, respectively.

The internal parameters for the $W_2Cl_6P_4$ cores of the PMe_3 and PEt_3 complexes are not surprisingly very similar and, together with the previously reported $W_2Cl_6N_4$ core of the pyridine adduct, form an interesting group of d^3–d^3 compounds. (1) The W–W distances span the narrow range of 2.71–2.74 Å. (2) The internal angles associated with the $W_2(\mu\text{-}Cl)_2$ moiety are acute at the bridging halogen, 70°, and obtuse at tungsten, 110°. (3) The tungsten to terminal ligand distances that lie in the plane of the $W_2(\mu\text{-}Cl)_2$ moiety are longer than those that are out of the plane. (4) The W–Cl distances associated with the bridging ligands are unusually short, 2.37–2.40 Å, and consistently shorter than the terminal W–Cl bonding in the $W_2(\mu\text{-}Cl)_2$ plane by more than 0.05 Å. A similar trend was seen for $W_2Cl_6(PMe_2Ph)_4$.[6]

Points 1 and 2 are clearly indicative of the importance of M–M bonding in these d^3–d^3 dinuclear compounds, and it is likely that points 3 and 4 also have their origin in a mixing of metal–metal and metal–ligand bonding. Indeed, it is only easy to formulate the M–M σ component to the M–M bond. There is extensive mixing of M–M π, δ, and δ^* with ligand-filled pπ orbitals. This has been noted in general for edge-shared bioctahedra,[8] and in the absence of a detailed MO calculation, we shall not speculate further on the origin of the trends noted in points 3 and 4 above.

The molecular structure of $W_2Cl_6(PEt_3)_3$ contains a central $W_2(\mu\text{-}Cl_3)$ core that is very similar to those seen in the $[W_2Cl_7(THF)_2]^-$ and $W_2Cl_9^{3-}$ anions.[4] The W–W distance is 2.47 Å, somewhat longer than in the other instances which fall at 2.41 Å, but it is still notably shorter than the distance found

(8) (a) Shaik, S.; Hoffmann, R.; Fisel, C. R.; Summerville, R. H. *J. Am. Chem. Soc.* **1980**, *102*, 4555. (b) Cotton, F. A. *Polyhedron* **1987**, *6*, 667. (c) Cotton, F. A.; Eglin, J. L.; Hong, B.; James, C. L. *J. Am. Chem. Soc.* **1992**, *114*, 4915. The compound $Mo_2Cl_6(PEt_3)_4$ is in fact paramagnetic with no Mo–Mo bond: Mui, H. D.; Poli, R. *Inorg. Chem.* **1989**, *28*, 3609; **1991**, *30*, 65.

Table III. Fractional Coordinates and Isotropic Thermal Parameters for $W_2Cl_6(PEt_3)_4$

atom	10^4x	10^4y	10^4z	$10B_{iso}$, Å^2
W(1)	5574.4(3)	2275.8(2)	5333.9(2)	10
W(2)	6981.5(3)	2663.7(2)	4305.1(2)	10
Cl(3)	4859(2)	2508(1)	4063(1)	13
Cl(4)	7726(2)	2450(1)	5559(1)	14
Cl(5)	5638(2)	982(1)	5208(1)	14
Cl(6)	5071(2)	3452(1)	5770(1)	14
Cl(7)	6708(2)	2969(1)	3002(1)	16
Cl(8)	9124(2)	2873(1)	4253(1)	15
P(9)	3263(2)	2100(1)	5300(1)	13
P(10)	6025(2)	1909(1)	6706(1)	14
P(11)	7407(2)	1394(1)	3829(1)	14
P(12)	6907(2)	4037(1)	4457(1)	12
C(13)	2285(9)	2519(6)	4546(5)	17
C(14)	2302(9)	3348(6)	4530(6)	20
C(15)	2751(9)	1165(6)	5209(5)	18
C(16)	2691(9)	857(6)	4443(6)	18
C(17)	2655(9)	2451(5)	6100(5)	16
C(18)	1294(9)	2417(7)	6082(5)	24
C(19)	5091(9)	1158(5)	6943(5)	17
C(20)	5308(10)	882(6)	7723(6)	25
C(21)	5808(10)	2624(6)	7367(5)	21
C(22)	6819(11)	3203(7)	7448(6)	30
C(23)	7559(10)	1597(6)	7048(6)	23
C(24)	7964(10)	905(7)	6720(6)	29
C(25)	8211(9)	746(5)	4474(6)	18
C(26)	9462(9)	1000(6)	4811(6)	21
C(27)	6115(9)	854(5)	3416(5)	16
C(28)	5380(9)	1175(6)	2733(6)	23
C(29)	8366(9)	1441(6)	3103(6)	20
C(30)	8828(11)	720(6)	2850(6)	28
C(31)	5431(9)	4470(5)	4254(5)	16
C(32)	4831(9)	4406(6)	3461(6)	21
C(33)	7808(10)	4507(6)	3848(6)	19
C(34)	7881(9)	5317(6)	3931(6)	21
C(35)	7503(9)	4420(5)	5360(5)	16
C(36)	8842(9)	4319(6)	5599(6)	23

Table IV. Fractional Coordinates and Isotropic Thermal Parameters for $W_2Cl_6(PEt_3)_3{\cdot}CH_2Cl_2$

atom	10^4x	10^4y	10^4z	$10B_{iso}$, Å
W(1)	9718.3(3)	9094.0(3)	7337.4(2)	9
W(2)	10454.4(3)	7464.7(3)	7009.9(2)	9
Cl(3)	11461(2)	9002(2)	7175(1)	12
Cl(4)	9584(2)	7549(2)	8086(1)	15
Cl(5)	9019(2)	8202(2)	6217(1)	14
Cl(6)	9748(2)	5805(2)	6793(2)	17
Cl(7)	10311(2)	9955(2)	8435(1)	18
Cl(8)	9665(2)	10645(2)	6663(1)	16
P(9)	7965(2)	9354(2)	7474(2)	15
P(10)	11143(2)	7246(2)	5825(2)	13
P(11)	11793(2)	6724(2)	7905(2)	13
C(12)	7306(8)	10281(9)	6848(7)	20
C(13)	7132(9)	9979(11)	6062(7)	28
C(14)	7786(9)	9952(11)	8331(7)	26
C(15)	8060(10)	9291(13)	8978(7)	37
C(16)	7268(8)	8181(10)	7384(6)	19
C(17)	6196(8)	8281(11)	7424(7)	24
C(18)	11676(8)	8388(9)	5463(6)	17
C(19)	10974(9)	9288(10)	5293(6)	23
C(20)	10200(8)	6817(9)	5102(6)	19
C(21)	10518(8)	6648(10)	4365(6)	20
C(22)	12098(8)	6297(10)	5785(6)	18
C(23)	11863(9)	5191(10)	5918(7)	24
C(24)	12973(8)	6547(9)	7627(6)	16
C(25)	13496(8)	7504(10)	7406(7)	26
C(26)	11566(8)	5423(9)	8246(6)	19
C(27)	10754(9)	5331(10)	8684(7)	25
C(28)	12034(8)	7527(9)	8715(6)	18
C(29)	12842(10)	7143(12)	9273(7)	31
C(30)	10138(11)	8257(12)	10151(8)	34
Cl(31)	11310(3)	7873(4)	10510(2)	48
Cl(32)	9308(4)	7239(4)	10158(3)	58

in the edge-shared bioctahedron. The W–Cl distances associated with the bridging groups are longer by ca. 0.1 Å than those

Table V. Fractional Coordinates and Isotropic Thermal Parameters for $[HPEt_3]^+[W_2Cl_7(PEt_3)_2]^-$

atom	10^4x	10^4y	10^4z	$10B_{iso}$, Å^2
W(1)	3921(1)	835.1(4)	2180(1)	21
W(2)	3502(1)	1466.2(5)	2754(1)	21
Cl(3)	3713(7)	1449(3)	1314(5)	22
Cl(4)	5351(7)	1095(2)	3486(5)	23
Cl(5)	2057(7)	917(3)	2543(6)	32
Cl(6)	4141(7)	234(3)	2975(5)	25
Cl(7)	2729(8)	529(3)	915(6)	32
P(8)	5696(8)	725(3)	1690(6)	23
C(9)	7009(30)	1017(10)	2189(22)	25(7)
C(10)	6795(32)	1466(11)	2037(23)	31(7)
C(11)	6236(38)	213(13)	1892(28)	45(9)
C(12)	5423(38)	-94(12)	1334(28)	45(9)
C(13)	5396(27)	798(10)	561(20)	19(6)
C(14)	6415(38)	725(13)	204(28)	46(9)
Cl(15)	4712(8)	2049(3)	2997(6)	30
Cl(16)	3261(8)	1528(4)	4121(6)	43
P(17)	1697(8)	1860(3)	2033(6)	26
C(18)	1988(35)	2381(12)	1802(26)	38(8)
C(19)	2516(39)	2424(13)	1165(29)	47(9)
C(20)	836(30)	1638(10)	1054(22)	25(7)
C(21)	-388(33)	1857(11)	645(24)	33(8)
C(22)	665(40)	1949(13)	2649(29)	50(9)
C(23)	172(44)	1588(14)	2915(31)	59(10)
W(24)	3823(1)	6685.9(4)	2247(1)	16
W(25)	4478(1)	6014.6(4)	2697(1)	21
Cl(26)	2853(7)	6105(2)	1382(5)	21
Cl(27)	3561(7)	6448(3)	3583(5)	24
Cl(28)	5934(7)	6503(3)	2550(6)	26
Cl(29)	4000(7)	6944(3)	968(5)	22
Cl(30)	4569(7)	7274(2)	3058(5)	19
P(31)	1748(7)	6942(3)	1823(6)	19
C(32)	1022(31)	6849(10)	707(22)	27(7)
C(33)	-227(38)	7004(13)	394(28)	45(9)
C(34)	1681(36)	7485(12)	1939(27)	39(8)
C(35)	2244(29)	7730(10)	1459(21)	22(6)
C(36)	782(28)	6749(9)	2384(20)	20(6)
C(37)	533(30)	6300(10)	2246(22)	26(7)
Cl(38)	3254(9)	5491(3)	2934(7)	35
Cl(39)	5978(10)	5840(4)	3969(7)	55
P(40)	5222(8)	5619(3)	1687(6)	22
C(41)	5193(32)	5911(11)	766(23)	31(7)
C(42)	5637(31)	5687(10)	90(22)	28(7)
C(43)	6671(32)	5406(10)	2083(23)	28(7)
C(44)	7716(39)	5735(13)	2279(28)	48(9)
C(45)	4319(34)	5189(11)	1281(25)	35(8)
C(46)	4484(36)	4818(12)	1812(26)	40(8)
P(47)	2559(10)	531(3)	4773(7)	35
C(48)	1171(33)	723(11)	4776(24)	35(8)

associated with the terminal W–Cl bonds, and bonds trans to the PEt_3 ligands are longer than those trans to W–Cl bonds as a result of the trans-influence order $PEt_3 > Cl^-$. Similar structural features were seen in $W_2X_6(PMe_2Ph)_3$, where X = Cl and Br.[6]

For $[HPEt_3]^+[W_2Cl_7(PEt_3)_2]^-$ there are two independent cation–anions in the unit cell. The structures of the two FSBO $[W_2Cl_7(PEt_3)_2]^-$ anions are shown in Figures 3 and 4. The cation–anion association for one is shown in Figure 5, and that of the other is essentially identical. There is evidently weak hydrogen bonding between four of the W–Cl bonds and the P–H group of the cation as indicated in Figure 5. Each W atom is coordinated to three bridging chloride ligands, two terminal chloride groups, and a terminal PEt_3 ligand. For a FSBO anion of formula $M_2X_7L_2$ there are two possible isomers for such a symmetrical disposition of ligands, namely syn and gauche isomers as diagramatically shown. The gauche isomer has two enantiomers, and in the

syn

gauche

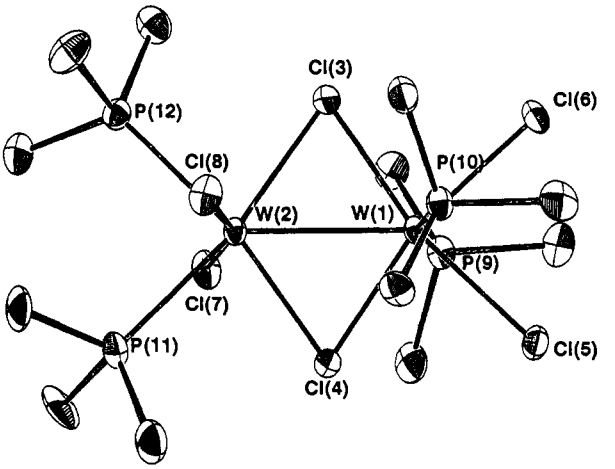

Figure 1. ORTEP drawing of the $W_2Cl_6(PMe_3)_4$ molecule showing the atom number scheme. A similar $W_2Cl_6P_4$ atom number scheme is used in the tables for the structurally related $W_2Cl_6(PEt_3)_4$ molecule.

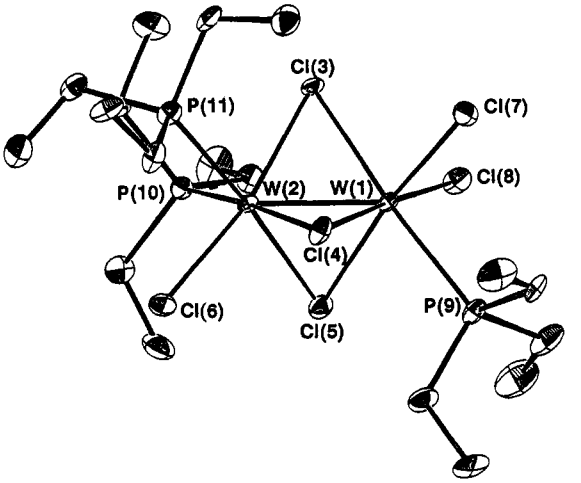

Figure 2. ORTEP drawing of the $W_2Cl_6(PEt_3)_3$ molecule showing the atom number scheme.

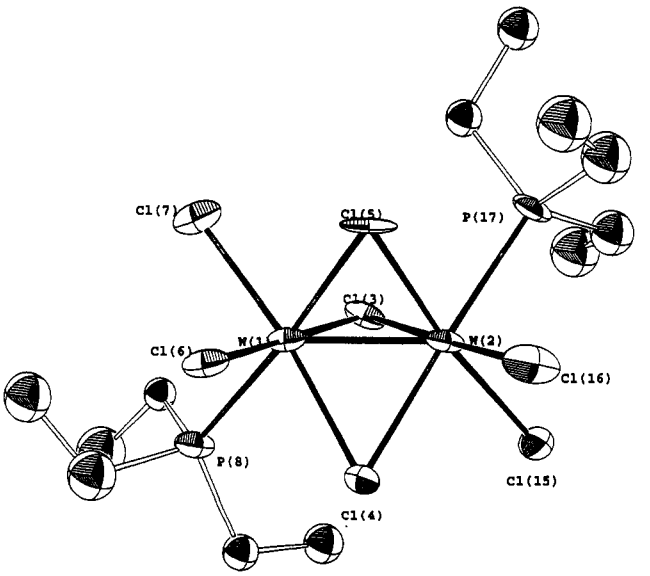

Figure 3. ORTEP drawing of one of the $[W_2Cl_7(PEt_3)_2]^-$ anions giving the atom number scheme.

structure of $[HPEt_3]^+[W_2Cl_7(PEt_3)_2]^-$ that is exactly what is found. The unit cell contains the enantiomeric pair of the *gauche*-$[W_2Cl_7(PEt_3)_2]^-$ anions. A similar situation was recently found for the salt $[HPMe_3]^+[Mo_2Cl_7(PMe_3)_2]^-$ by Cotton and

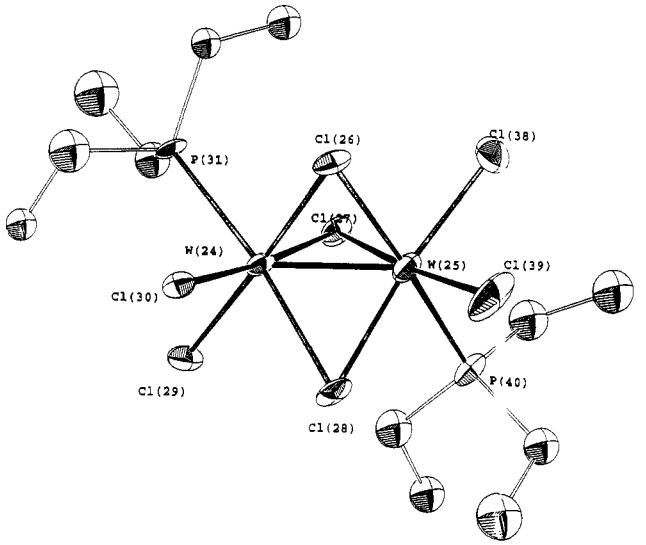

Figure 4. ORTEP drawing of the other $[W_2Cl_7(PEt_3)_2]^-$ anion found in the unit cell of the $[HPEt_3]^+[W_2Cl_7(PEt_3)_2]^-$ salt showing its atom number scheme.

Luck.[9] In the iodo salts $(cat^+)[Mo_2I_7(PMe_3)_2]^-$, where cat = $HPMe_3$, Me_4N, and Ph_4As, the anti isomer was structurally characterized by Cotton and Poli.[10]

The W–W distances in the FSBO $[W_2Cl_7(PEt_3)_2]^-$ anions are short, 2.43 Å, and comparable to those in the $W_2Cl_6L_3$ compounds reported in this work and elsewhere.[6] The W–Cl distances associated with the bridges are longer than the W–Cl terminal groups, and those bridging W–Cl bonds that are trans to the terminal W–PEt_3 bonds are slightly longer than the other W–Cl bridging distances.

Solution Behavior—NMR Studies of the Equilibrium 4. The compounds have been characterized by variable-temperature ^1H and $^{31}P\{^1H\}$ NMR spectroscopy and the equilibrium, eq 4, has been monitored as a function of time and temperature.

The ^{31}P spectra of $W_2Cl_6L_4$ compounds show two broad ^{31}P signals assignable to the axial and equatorial W–PR_3 ligands. The chemical shifts of the ^{31}P resonances shift quite dramatically to higher field with increasing temperature as shown in Figure 6. The change in chemical shift from −90 to +22 °C is more than 100 ppm. This we believe arises from the relatively low-lying excited states in the M–M $\delta\delta^*\pi^*$ manifold, which generate a temperature dependent paramagnetic contribution to the chemical shift.[8c] Above +30 °C the $W_2Cl_6L_4$ compounds are not detectable by NMR spectroscopy because the equilibrium lies in favor of $W_2Cl_6L_3$ and free L when L = PEt_3 and $P(n\text{-}Bu)_3$. When L = PMe_3, the $W_2Cl_6(PMe_3)_4$ compound is favored in the temperature range −80 to +75 °C in toluene-d_8. The difference between the stability of the $W_2Cl_6L_4$ complexes is presumably influenced by steric factors which favor dissociation of $PEt_3 > PMe_3$.

The ^{31}P NMR spectra of the $W_2Cl_6L_3$ compound shows two ^{31}P signals in the integral ratio 2:1 and appear as doublets and 1:2:1 triplets, respectively, due to ^{31}P–^{31}P coupling. The structure of $W_2Cl_6(PEt_3)_3$ has a virtual mirror plane of symmetry such that the PEt_3 ligands represented by P(11) and P(10) in Figure 3 are equivalent. Evidently this isomer is present in solution since a FSBO molecule in which say P(11) and Cl(6) were exchanged would have three inequivalent PEt_3 ligands.

Two different samples of $W_2Cl_6(PEt_3)_4$ were prepared in toluene-d_8, and the equilibrium concentrations of $W_2Cl_6(PEt_3)_4$ and $W_2Cl_6(PEt_3)_3$ were estimated by ^{31}P NMR spectroscopy over the temperature range +22 to −15 °C. From these measurements we have determined K_{eq} for eq 4 and by a plot of ln K_{eq} vs $1/T$ we have obtained $\Delta H° = -2.5$ (±0.5) kcal mol^{-1} and $\Delta S° = -4$ (±2) eu. We find that the $W_2Cl_6(PEt_3)_4$ compound is enthalpically favored while the $W_2Cl_6(PEt_3)_3$ and free PEt_3 are favored by entropy. However, the magnitude of both $\Delta H°$ and $\Delta S°$ are notably small which leads to a *relatively* small concentration dependence of the equilibrium with temperature when compared to an equilibrium involving $Mo_2(OR)_6$ and $Mo_2(OR)_6(PR_3)_2$, eq 7.[11]

$$M_2(OR)_6L_2 \rightleftarrows M_2(OR)_6 + 2L \qquad (7)$$

$$M = Mo, W; L = PMe_3$$

Studies of eq 7 reveal $\Delta H° \sim +15$ kcal mol^{-1} and $\Delta S° \approx +30$ eu, which is more typical of a reaction wherein a metal–ligand bond is being reversibly broken.

The small value of $\Delta H°$ in eq 4 is presumably a reflection of the internal compensation of metal–metal and metal–ligand bonding that accompanies the interconversion of FSBO and ESBO d^3–d^3 dimers. So, although a new W–PEt_3 bond is formed upon addition of PEt_3 to $W_2Cl_6(PEt_3)_3$, which one might surely think to be worth ≥20 kcal mol^{-1}, the W–W distance increases from 2.44 to 2.72 Å and one chloride bridge is broken. Conversely, when one W–PEt_3 bond is broken in the conversion of $W_2Cl_6(PEt_3)_4$ to $W_2Cl_6(PEt_3)_3$ and free PEt_3, the W–W bonding increases as the W–W distance contracts by 0.3 Å and an additional tungsten chloride bridge is formed. Enthalpically, the system is buffered by metal–metal and metal–ligand bonding.

It is perhaps more difficult to interpret the relatively small value of $\Delta S°$ since we are not sure of the solvation effects of the $W_2Cl_6(PEt_3)_4$ and $W_2Cl_6(PEt_3)_3$ compounds. Just on the basis of the bimolecular nature of the reaction, one would anticipate the formation of $W_2Cl_6(PEt_3)_4$ from $W_2Cl_6(PEt_3)_3$ and free PEt_3 would involve the loss of ca. 30 eu. However, it is possible that the $W_2Cl_6(PEt_3)_3$ molecule is somewhat more solvated and thus in the conversion to $W_2Cl_6(PEt_3)_4$ there is a favorable entropy of solvation. An extreme case of the importance of solvation is seen in the equilibrium involving *cis*- and *trans*-$(PR_3)_2PtCl_2$ compounds in benzene where the isomerization cis → trans is favored by an estimated release of ca. 3 molecules of benzene.[12] We might not expect such a dramatic effect for the $W_2Cl_6(PEt_3)_4$ and $W_2Cl_6(PEt_3)_3$ compounds, but the dipole moments of the two compounds are not known. Moreover, the internal degrees of freedom of the FSBO complex must be less than that of the ESBO complex because of the greater number of bridging bonds.

The kinetics of equilibrium 4 were estimated by the following procedure. Samples of $W_2Cl_6(PEt_3)_4$ dissolved in toluene-d_8 in the presence of an excess of PEt_3 were heated to 60–65 °C. This drove the equilibrium in favor of $W_2Cl_6(PEt_3)_3$ and free PEt_3. The samples were then cooled to X °C (where $+22 > X > -15$) and the approach to equilibrium was monitored with time. The relative concentrations of the $W_2Cl_6(PEt_3)_3$ and $W_2Cl_6(PEt_3)_4$ complexes were estimated by integration of the ^{31}P signals.

The first thing that was apparent from this study was that the formation of $W_2Cl_6(PEt_3)_4$ from $W_2Cl_6(PEt_3)_3$ and free PEt_3 (present in an excess) is dependent on $[PEt_3]$. The rate of formation of $W_2Cl_6(PEt_3)_4$ does not show saturation kinetics even at large $[PEt_3]$. This clearly indicates that $W_2Cl_6(PEt_3)_3$ is susceptible to nucleophilic attack by the entering PEt_3 ligand. The stereospecific nature of the reaction requires that the chloride bridge trans to the PEt_3 ligand at the monophosphine substituted

(9) Cotton, F. A.; Luck, R. L. *Inorg. Chem.* **1989**, *28*, 182.
(10) Cotton, F. A.; Poli, R. *Inorg. Chem.* **1987**, *26*, 3310.
(11) Chisholm, M. H.; Hampden-Smith, M. J. Proceedings of the 19th ACS Regional Meeting, Columbus, OH, June 1987.
(12) Basolo, F.; Pearson, R. G. In *Mechanisms of Inorganic Reactions*, 2nd ed.; J. Wiley and Sons Publishers: New York, 1967.

Table VI. Selected Bond Distances (Å) and Angles (deg) for $W_2Cl_6(PMe_3)_4$ (I) and $W_2Cl_6(PEt_3)_4$ (II)

Bond Distances

	I	II		I	II
W(1)–W(2)	2.7113(8)	2.7397(7)	W(2)–Cl(3)	2.4096(24)	2.4129(23)
W(1)–Cl(3)	2.3874(24)	2.3762(23)	W(2)–Cl(4)	2.4067(25)	2.4107(23)
W(1)–Cl(4)	2.3716(25)	2.3842(23)	W(2)–Cl(7)	2.4130(25)	2.4023(24)
W(1)–Cl(5)	2.4676(25)	2.4509(24)	W(2)–Cl(8)	2.4136(25)	2.4126(24)
W(1)–Cl(6)	2.4561(25)	2.4538(24)	W(2)–P(11)	2.5551(27)	2.6072(26)
W(1)–P(9)	2.5270(26)	2.5727(27)	W(2)–P(12)	2.5804(27)	2.6053(26)
W(1)–P(10)	2.5248(26)	2.5540(26)	P(9)–C(16)	1.822(12)	

P–C = 1.82 (av)

Bond Angles

	I	II		I	II
W(2)–W(1)–Cl(3)	55.97(6)	55.74(6)	W(1)–W(2)–Cl(4)	54.82(6)	54.70(6)
W(2)–W(1)–Cl(4)	56.04(6)	55.61(6)	W(1)–W(2)–Cl(7)	100.51(7)	99.46(6)
W(2)–W(1)–Cl(5)	137.23(6)	137.40(6)	W(1)–W(2)–Cl(8)	100.46(7)	100.59(6)
W(2)–W(1)–Cl(6)	136.67(6)	137.85(6)	W(1)–W(2)–P(11)	133.93(6)	134.07(6)
W(2)–W(1)–P(9)	98.87(7)	98.89(6)	W(1)–W(2)–P(12)	134.82(6)	133.44(6)
W(2)–W(1)–P(10)	98.56(7)	98.72(6)	Cl(3)–W(2)–Cl(4)	110.01(8)	109.17(8)
Cl(3)–W(1)–Cl(4)	112.01(8)	111.35(8)	Cl(3)–W(2)–Cl(7)	92.88(9)	95.30(8)
Cl(3)–W(1)–Cl(5)	166.67(8)	166.83(8)	Cl(3)–W(2)–Cl(8)	98.38(9)	96.06(8)
Cl(3)–W(1)–Cl(6)	80.75(8)	82.12(8)	Cl(3)–W(2)–P(11)	168.86(8)	170.77(8)
Cl(3)–W(1)–P(9)	96.81(9)	93.20(8)	Cl(3)–W(2)–P(12)	79.96(9)	79.00(8)
Cl(3)–W(1)–P(10)	93.89(9)	95.32(8)	Cl(4)–W(2)–Cl(7)	99.80(9)	96.12(8)
Cl(4)–W(1)–Cl(5)	81.20(9)	81.81(8)	Cl(4)–W(2)–Cl(8)	92.93(9)	95.69(8)
Cl(4)–W(1)–Cl(6)	167.15(9)	166.46(8)	Cl(4)–W(2)–P(11)	79.55(9)	79.51(8)
Cl(4)–W(1)–P(9)	93.77(9)	97.30(8)	Cl(4)–W(2)–P(12)	168.17(9)	171.49(8)
Cl(4)–W(1)–P(10)	94.98(9)	93.99(8)	Cl(7)–W(2)–Cl(8)	159.02(9)	159.95(8)
Cl(5)–W(1)–Cl(6)	86.10(9)	84.75(8)	Cl(7)–W(2)–P(11)	79.54(9)	80.33(8)
Cl(5)–W(1)–P(9)	83.67(9)	84.16(8)	Cl(7)–W(2)–P(12)	85.66(9)	85.24(8)
Cl(5)–W(1)–P(10)	82.76(9)	84.03(8)	Cl(8)–W(2)–P(11)	86.53(9)	85.96(8)
Cl(6)–W(1)–P(9)	82.80(9)	82.83(8)	Cl(8)–W(2)–P(12)	79.00(9)	80.79(8)
Cl(6)–W(1)–P(10)	85.33(9)	83.02(8)	P(11)–W(2)–P(12)	91.25(9)	92.48(8)
P(9)–W(1)–P(10)	162.53(9)	162.31(8)	W(1)–Cl(3)–W(2)	68.83(7)	69.79(6)
W(1)–W(2)–Cl(3)	55.20(6)	54.48(6)	W(1)–Cl(4)–W(2)	69.14(7)	69.69(6)

metal center is the one that is broken as shown diagramatically in eq 8.

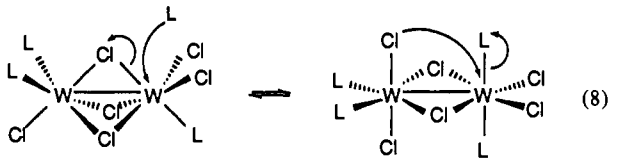

(8)

From studies of the rate of formation of $W_2Cl_6(PEt_3)_4$ as a function of temperature in the presence of excess phosphine (pseudo-first-order conditions), we can estimate the activation parameters for the associative reaction: $\Delta H^{\ddagger} = 8 \pm 1$ kcal mol^{-1} and $\Delta S^{\ddagger} = -50 \pm 8$ eu. We cannot establish these values to a high degree of accuracy by employing the NMR method. Integration of ^{31}P signals introduces potentially significant errors. However, the relative magnitude of these parameters is more meaningful anyway because eq 4, although specifically stated for L = PEt_3, is much more general in nature. Thus the small positive value of $\Delta H^{\ddagger}$ and the relatively large negative value for $\Delta S^{\ddagger}$ are taken to serve as an indicator of the associative nature of the formation of $W_2Cl_6(PEt_3)_4$ from the FSBO complex and free ligand. The magnitude of $\Delta H^{\ddagger}$ and $\Delta S^{\ddagger}$ are very similar to those recently reported by Poë and co-workers[13] for the associative phosphine for carbonyl substitution reaction involving $Ru_6(\mu_6\text{-}C)(CO)_{17}$ and $P(p\text{-}X\text{-}C_6H_4)_3$, where X = H, OMe, Me, Cl, and CF_3.

General Comments on the Interconversion of FSBO and ESBO Complexes. Cotton et al. recently[14] examined the phosphine attack on dirhodium FSBO complexes. The attack on the non-M–M-bonded $Rh_2Cl_6L_3$ dimers yielded initially ESBO $Rh_2Cl_6L_4$ compounds, and then by further phosphine association and cleavage of the chloride bridges *mer*-$RhCl_3L_3$ were formed. These

(13) Poë, A. J.; Farrar, D. H.; Zheng, Y. *J. Am. Chem. Soc.* **1992**, *114*, 5146.
(14) Cotton, F. A.; Eglin, J. L.; Kang, S. J. *J. Am. Chem. Soc.* **1992**, *114*, 405.

Table VII. Pertinent Bond Distances (Å) and Angles (deg) for $W_2Cl_6(PEt_3)_3 \cdot CH_2Cl_2$

Bond Distances

W(1)–W(2)	2.4705(7)	W(2)–Cl(4)	2.5093(27)
W(1)–Cl(3)	2.5193(25)	W(2)–Cl(5)	2.5274(26)
W(1)–Cl(4)	2.4718(27)	W(2)–Cl(6)	2.3842(28)
W(1)–Cl(5)	2.4829(27)	W(2)–P(10)	2.564(3)
W(1)–Cl(7)	2.3925(27)	W(2)–P(11)	2.536(3)
W(1)–Cl(8)	2.3732(28)	Cl(31)–C(30)	1.767(16)
W(1)–P(9)	2.541(3)	Cl(32)–C(30)	1.765(16)
W(2)–Cl(3)	2.4427(26)	P(9)–C(12)	1.840(12)

P–C = 1.83 (av)

Bond Angles

W(2)–W(1)–Cl(3)	58.61(6)	W(1)–W(2)–Cl(5)	59.56(6)
W(2)–W(1)–Cl(4)	61.02(6)	W(1)–W(2)–Cl(6)	129.49(7)
W(2)–W(1)–Cl(5)	61.36(6)	W(1)–W(2)–P(10)	122.24(7)
W(2)–W(1)–Cl(7)	120.41(7)	W(1)–W(2)–P(11)	117.31(7)
W(2)–W(1)–Cl(8)	125.17(7)	Cl(3)–W(2)–Cl(4)	101.66(9)
W(2)–W(1)–P(9)	125.92(7)	Cl(3)–W(2)–Cl(5)	99.72(9)
Cl(3)–W(1)–Cl(4)	100.57(9)	Cl(3)–W(2)–Cl(6)	168.81(9)
Cl(3)–W(1)–Cl(5)	98.86(9)	Cl(3)–W(2)–P(10)	85.27(9)
Cl(3)–W(1)–Cl(7)	84.08(9)	Cl(3)–W(2)–P(11)	81.95(9)
Cl(3)–W(1)–Cl(8)	86.26(9)	Cl(4)–W(2)–Cl(5)	91.01(9)
Cl(3)–W(1)–P(9)	174.95(9)	Cl(4)–W(2)–Cl(6)	86.44(9)
Cl(4)–W(1)–Cl(5)	92.96(9)	Cl(4)–W(2)–P(10)	172.17(9)
Cl(4)–W(1)–Cl(7)	86.17(10)	Cl(4)–W(2)–P(11)	83.34(9)
Cl(4)–W(1)–Cl(8)	172.88(9)	Cl(5)–W(2)–Cl(6)	87.72(9)
Cl(4)–W(1)–P(9)	84.15(9)	Cl(5)–W(2)–P(10)	84.18(9)
Cl(5)–W(1)–Cl(7)	177.04(9)	Cl(5)–W(2)–P(11)	174.33(9)
Cl(5)–W(1)–Cl(8)	87.91(9)	Cl(6)–W(2)–P(10)	91.46(10)
Cl(5)–W(1)–P(9)	82.57(9)	Cl(6)–W(2)–P(11)	87.20(10)
Cl(7)–W(1)–Cl(8)	92.61(10)	P(10)–W(2)–P(11)	101.39(9)
Cl(7)–W(1)–P(9)	94.52(10)	W(1)–Cl(3)–W(2)	59.70(6)
Cl(8)–W(1)–P(9)	88.96(9)	W(1)–Cl(4)–W(2)	59.46(6)
W(1)–W(2)–Cl(3)	61.69(6)	W(1)–Cl(5)–W(2)	59.08(6)
W(1)–W(2)–Cl(4)	59.51(6)		

Table VIII. Bond Distances (Å) and Angles (deg) for $[HPEt_3]^+[W_2Cl_7(PEt_3)_2]^-$

Bond Distances

W(1)–W(2)	2.4377(22)	W(24)–Cl(26)	2.492(8)
W(1)–Cl(3)	2.485(8)	W(24)–Cl(27)	2.475(8)
W(1)–Cl(4)	2.486(9)	W(24)–Cl(28)	2.506(8)
W(1)–Cl(5)	2.506(9)	W(24)–Cl(29)	2.373(8)
W(1)–Cl(6)	2.382(8)	W(24)–Cl(30)	2.405(8)
W(1)–Cl(7)	2.392(9)	W(24)–P(31)	2.524(8)
W(1)–P(8)	2.532(9)	W(25)–Cl(26)	2.471(8)
W(2)–Cl(3)	2.492(8)	W(25)–Cl(27)	2.549(8)
W(2)–Cl(4)	2.514(8)	W(25)–Cl(28)	2.463(8)
W(2)–Cl(5)	2.481(9)	W(25)–Cl(38)	2.398(9)
W(2)–Cl(15)	2.395(9)	W(25)–Cl(39)	2.401(10)
W(2)–Cl(16)	2.394(9)	W(25)–P(40)	2.512(9)
W(2)–P(17)	2.511(9)	P(8)–C(9)	1.83(4)
W(24)–W(25)	2.4271(21)		

P–C = 1.81 (av)

Bond Angles

W(2)–W(1)–Cl(3)	60.82(20)	W(25)–W(24)–Cl(29)	120.47(21)
W(2)–W(1)–Cl(4)	61.40(19)	W(25)–W(24)–Cl(30)	123.83(21)
W(2)–W(1)–Cl(5)	60.23(23)	W(25)–W(24)–P(31)	126.98(21)
W(2)–W(1)–Cl(6)	121.14(24)	Cl(26)–W(24)–Cl(27)	96.0(3)
W(2)–W(1)–Cl(7)	125.41(25)	Cl(26)–W(24)–Cl(28)	101.03(27)
W(2)–W(1)–P(8)	123.21(23)	Cl(26)–W(24)–Cl(29)	85.3(3)
Cl(3)–W(1)–Cl(4)	98.0(3)	Cl(26)–W(24)–Cl(30)	174.35(26)
Cl(3)–W(1)–Cl(5)	96.3(3)	Cl(26)–W(24)–P(31)	81.70(27)
Cl(3)–W(1)–Cl(6)	178.0(3)	Cl(27)–W(24)–Cl(28)	97.9(3)
Cl(3)–W(1)–Cl(7)	85.1(3)	Cl(27)–W(24)–Cl(29)	176.8(3)
Cl(3)–W(1)–P(8)	83.0(3)	Cl(27)–W(24)–Cl(30)	83.5(3)
Cl(4)–W(1)–Cl(5)	100.3(3)	Cl(27)–W(24)–P(31)	88.7(3)
Cl(4)–W(1)–Cl(6)	83.1(3)	Cl(28)–W(24)–Cl(29)	84.7(3)
Cl(4)–W(1)–Cl(7)	173.0(3)	Cl(28)–W(24)–Cl(30)	84.62(27)
Cl(4)–W(1)–P(8)	84.8(3)	Cl(28)–W(24)–P(31)	172.5(3)
Cl(5)–W(1)–Cl(6)	85.1(3)	Cl(29)–W(24)–Cl(30)	94.9(3)
Cl(5)–W(1)–Cl(7)	85.5(3)	Cl(29)–W(24)–P(31)	88.6(3)
Cl(5)–W(1)–P(8)	174.9(3)	Cl(30)–W(24)–P(31)	92.7(3)
Cl(6)–W(1)–Cl(7)	93.6(3)	W(24)–W(25)–Cl(26)	61.16(19)
Cl(6)–W(1)–P(8)	95.5(3)	W(24)–W(25)–Cl(27)	59.58(20)
Cl(7)–W(1)–P(8)	89.4(3)	W(24)–W(25)–Cl(28)	61.66(19)
W(1)–W(2)–Cl(3)	60.52(20)	W(24)–W(25)–Cl(38)	124.91(24)
W(1)–W(2)–Cl(4)	60.24(20)	W(24)–W(25)–Cl(39)	125.8(3)
W(1)–W(2)–Cl(5)	61.25(23)	W(24)–W(25)–P(40)	115.49(22)
W(1)–W(2)–Cl(15)	125.98(23)	Cl(26)–W(25)–Cl(27)	94.63(27)
W(1)–W(2)–Cl(16)	123.3(3)	Cl(26)–W(25)–Cl(28)	102.9(3)
W(1)–W(2)–P(17)	121.32(24)	Cl(26)–W(25)–Cl(38)	83.0(3)
Cl(3)–W(2)–Cl(4)	97.07(27)	Cl(26)–W(25)–Cl(39)	172.7(4)
Cl(3)–W(2)–Cl(5)	96.8(3)	Cl(26)–W(25)–P(40)	79.37(28)
Cl(3)–W(2)–Cl(15)	87.0(3)	Cl(27)–W(25)–Cl(28)	97.1(3)
Cl(3)–W(2)–Cl(16)	176.2(3)	Cl(27)–W(25)–Cl(38)	85.8(3)
Cl(3)–W(2)–P(17)	82.9(3)	Cl(27)–W(25)–Cl(39)	88.1(3)
Cl(4)–W(2)–Cl(5)	100.2(3)	Cl(27)–W(25)–P(40)	173.8(3)
Cl(4)–W(2)–Cl(15)	85.4(3)	Cl(28)–W(25)–Cl(38)	173.2(3)
Cl(4)–W(2)–Cl(16)	85.7(3)	Cl(28)–W(25)–Cl(39)	83.4(4)
Cl(4)–W(2)–P(17)	177.9(3)	Cl(28)–W(25)–P(40)	82.9(3)
Cl(5)–W(2)–Cl(15)	172.7(3)	Cl(38)–W(25)–Cl(39)	90.5(4)
Cl(5)–W(2)–Cl(16)	85.3(3)	Cl(38)–W(25)–P(40)	94.9(3)
Cl(5)–W(2)–P(17)	81.8(3)	Cl(39)–W(25)–P(40)	98.0(3)
Cl(15)–W(2)–Cl(16)	90.6(4)	W(1)–Cl(3)–W(2)	58.66(19)
Cl(15)–W(2)–P(17)	92.5(3)	W(1)–Cl(4)–W(2)	58.36(19)
Cl(16)–W(2)–P(17)	94.2(3)	W(1)–Cl(5)–W(2)	58.52(18)
W(25)–W(24)–Cl(26)	60.29(19)	W(24)–Cl(26)–W(25)	58.55(19)
W(25)–W(24)–Cl(27)	62.67(20)	W(24)–Cl(27)–W(25)	57.75(17)
W(25)–W(24)–Cl(28)	59.87(21)	W(24)–Cl(28)–W(25)	58.47(18)

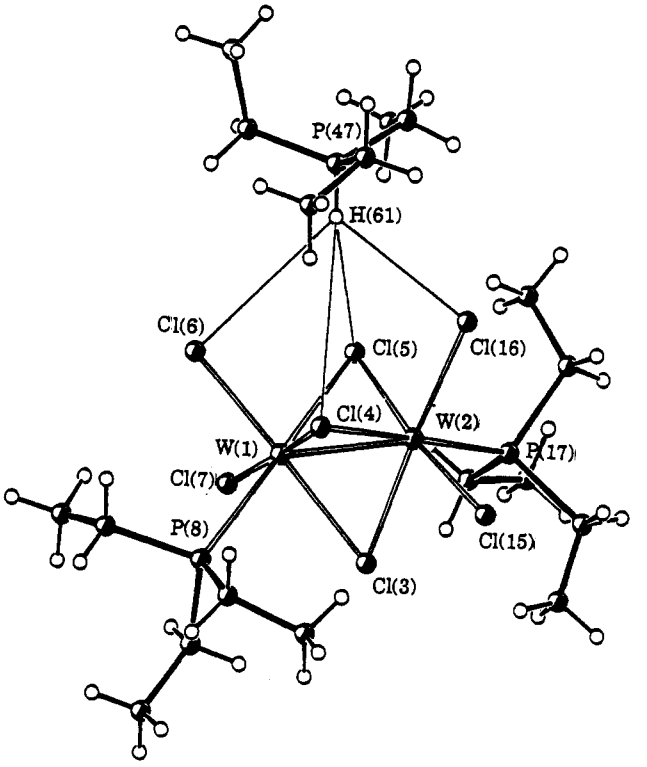

Figure 5. Ball-and-stick drawing of the $[HPEt_3]^+[W_2Cl_7(PEt_3)_2]^-$ salt showing the hydrogen bonding between the phosphonium cation and four of the chloride ligands of the anion.

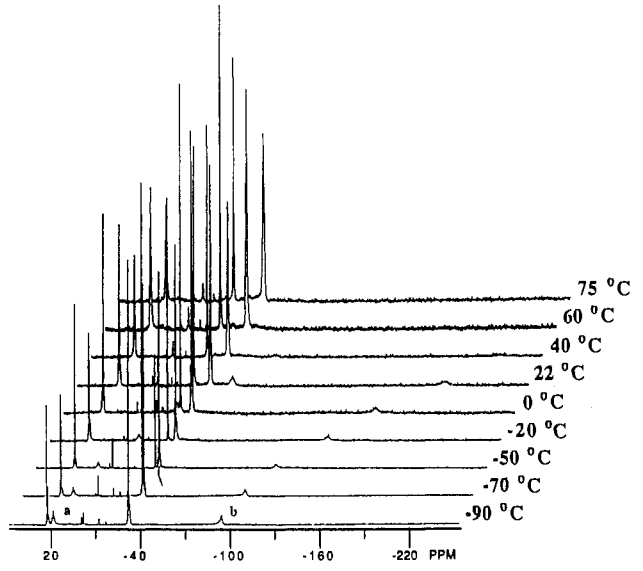

Figure 6. Variable-temperature $^{31}P\{^1H\}$ NMR spectrum of the equilibrium mixture of $W_2Cl_6(PEt_3)_4$ (marked a and b) and $W_2Cl_6(PEt_3)_3$ and free phosphine. Note the large chemical shift changes of a and b with increasing temperature.

reactions were noted to be stereospecific. The first reaction which generates the ESBO complex is stereochemically the same as that in eq 8. However, these workers did not examine the rate dependence on concentration of entering L. Since the rhodium dimers have no metal–metal bonds (the d^6–d^6 interaction would yield a M–M configuration of $\sigma^2\pi^4\pi^{*4}\sigma^{*2}$), the reaction mechanism may be rather different from that of eq 4 in its elementary form. Typically mononuclear octahedral rhodium(III) complexes with a t_{2g}^6 configuration are substitutionally inert and react by a dissociative or interchange–dissociative mechanism.[12] That is to say bond breaking is more important than bond making. In the case of a chloride-bridged dirhodium(III,III) complex we might expect that chloride bridge opening would be more facile than for a discrete mononuclear Rh(III) complex because one metal atom essentially assists in the cleavage of the bridge as pictorially represented by eq 9. The weakening of metal–halide bonds by

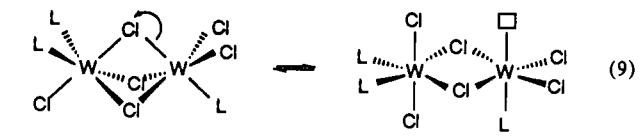

(9)

the introduction of ions that can coordinate to the halide is well-known in substitution chemistry and forms the basis of specific

ion catalysis, e.g., for $Co(NH_3)_5Cl^{2+} + H_2O(aq) \rightarrow Co(NH_3)_5(OH_2)^{3+} + Cl^-$, the use of Hg^{2+}.[15]

We mention this merely to draw attention to the fact that our observations concerning the interconversion of FSBO and ESBO complexes may not be general. Indeed, we would expect that the intimate mechanism will reflect the nature of the M···M interaction. For M = W and $d^n = d^3$, a relatively strong M–M bonding interaction facilitates the associative process because there are low-lying M–M π^* orbitals, but cleavage to mononuclear compounds does not occur. The latter would require rupture of all M–M bonding.

The compound $WCl_3(PMe_2Ph)_3$ was recently prepared and structurally characterized.[16] It is to our knowledge only the second structurally characterized mononuclear tungsten(III), t_{2g}^3 complex.[17] Cotton and Mandal[6] recently reported the synthesis of $W_2Cl_6(PMe_2Ph)_3$ and $W_2Cl_6(PMe_2Ph)_4$ and noted their inability to cleave the ESBO complex to the mononuclear compound WCl_3L_3 in the presence of excess phosphine. It is thus evident that there is a significant kinetic barrier for the reaction shown in eq 10.

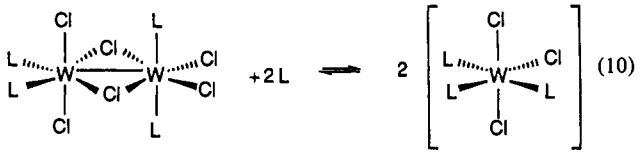

(10)

There are in fact good reasons to expect that the kinetic barrier for eq 10 would be large even though we do not know the values of $\Delta H°$ and $\Delta S°$. (1) The mononuclear W(3+), t_{2g}^3 complex would be substitutionally inert (as for Cr(3+)).[12] Dimerization via chloride bridge formation would not be kinetically labile, and dissociation of a W–L or W–Cl bond is enthalpically unfavorable. [Perhaps with a very bulky phosphine ligand, e.g. P(cyclohexyl)$_3$, this dissociation of PR_3 would become more facile. In a nonpolar hydrocarbon solvent dissociation of chloride is most unlikely.] (2) Although we would predict that the d^3–d^3 ESBO complex would be labile to an associative attack by L on electronic grounds, the formation of the mononuclear complex requires both the addition of *two* L and the rupture of the M–M bond.

Formation of the $[W_2Cl_7(PEt_3)_2]^-$ Anion. Working in hydrocarbon solvents, we find that this anion is formed from the equilibrium involving the FSBO and ESBO complexes, eq 4, when chloride ion is present. The thermodynamic stability of this anion probably reflect(s) the position of equilibrium 11 in nonpolar and

$$W_2Cl_6L_3 + Cl^- \rightleftarrows W_2Cl_7L_2^- + L \qquad (11)$$

non-hydrogen-bonding solvents. The chloride anion is a powerful nucleophile in a solvent such as benzene and the solvation of $[W_2Cl_7L_2]^-$ relative to Cl^- is probably favored entropically. This leads us back to note that if $W_2Cl_6(THF)_4$ and $W_2Cl_6(THF)_3$ could be formed then reaction with chloride ion would be favorable to give $[W_2Cl_7(THF)_2]^-$, which apparently is the species present in both THF and CH_2Cl_2 solvents.

Concluding Remarks

The addition of PR_3 (≥4 equiv) to a solution of $NaW_2Cl_7(THF)_5$ in tetrahydrofuran leads to the formation of $W_2Cl_6L_4$ compounds, where L = PMe_3, PEt_3, and $P(n\text{-}Bu)_3$. NaCl is formed in this reaction and, being very sparingly soluble in THF, is precipitated from solution. This is evidently important since in the presence of the soluble chloride ion source $[HPEt_3]^+Cl^-$ in hydrocarbon solvents the salt $[HPEt_3]^+[W_2Cl_7(PEt_3)_2]^-$ is formed from the equilibrium involving $W_2Cl_6(PEt_3)_4$ and $W_2Cl_6(PEt_3)_3$ and free PEt_3. Studies of the latter equilibrium show that the thermodynamic parameters $\Delta H°$ and $\Delta S°$ are small, specifically $\Delta H° = -2.5(\pm 0.5)$ kcal mol^{-1} (in favor of $W_2Cl_6(PEt_3)_4$) and $\Delta S° = -4(\pm 2)$ eu. The small values are proposed to reflect the internal buffering (compensation) of metal–ligand and metal–metal bonding. From studies of the rate of formation of $W_2Cl_6(PEt_3)_4$ from $W_2Cl_6(PEt_3)_3$ and free PEt_3, we observe a bimolecular reaction. The $W_2Cl_6(PEt_3)_3$ compound is therefore shown to be susceptible to nucleophilic attack by the entering PEt_3 ligand. These studies provide the first insights into the intimate mechanisms whereby d^3–d^3 edge- and face-shared bioctahedra are interconverted. The reader may care to note some related studies involving FSBO and ESBO $Mo_2Cl_6L_n$ (n = 3 or 4) complexes have recently been reported though thermodynamic and activation parameters were not determined in this work.[18]

Experimental Section

General Procedures. All procedures were carried out under dry nitrogen atmosphere by using standard Schlenk and glovebox techniques. Solvents were distilled from sodium benzophenone ketyl, with the exception of dichloromethane, which was distilled from calcium hydride, and stored under nitrogen over 4-Å molecular sieves. $NaW_2Cl_7(THF)_5$ was prepared according to previously published procedures.[3] Phosphines were obtained from Aldrich and degassed by three freeze–pump–thaw cycles.

^1H and $^{31}P\{^1H\}$ NMR spectra were obtained on a Nicolet NT-360 spectrometer at 360.07 and 146.16 MHz, respectively, and referenced to the residual solvent protons relative to TMS and to external 85% H_3PO_4 respectively. $^{13}C\{^1H\}$ NMR spectra were obtained on a Bruker AM-500 spectrometer and referenced to solvent carbon nuclei relative to TMS. Infrared spectra were obtained on a Perkin-Elmer 283 spectrophotometer as Nujol mulls between CsI plates or as a KBr disc with the exception of $[HPEt_3]^+[W_2Cl_7(PEt_3)_2]^-$. This was a KBr disk on a Nicolet S10P FTIR spectrometer. Elemental analyses were obtained from Oneida Research Services Inc., Whitesboro, NY.

Preparation of $W_2Cl_6(PMe_3)_4$.[3b,6] $NaW_2Cl_7(THF)_5$ (0.66 g, 0.66 mmol) was dissolved in THF (30 mL) in a 50-mL Schlenk flask equipped with a Teflon-coated stir bar and cooled to −196 °C with liquid nitrogen. The flask was evacuated and PMe_3 (2.7 mmol) was transferred with a calibrated gas line; the solution was allowed to warm to room temperature, nitrogen was allowed into the flask, and the solution was stirred for 15 h. The color of the solution changed from dark green to dark red-purple. The solution was filtered and the solvent removed in vacuo. The residue was redissolved in CH_2Cl_2 (10 mL) and layered with Et_2O (10 mL) and allowed to diffuse at room temperature for 15 h. The solution was cooled to −10 °C for an additional 2 days after which a first crop of red-purple crystals (145 mg, 0.164 mmol) was obtained. The supernatant was allowed to crystallize further at −10 °C, and a second crop of crystals was obtained (122 mg, 0.138 mmol) for an overall yield of 45%.

^1H NMR (21 °C, $CDCl_3$, δ): 1.43 (s, 18, PMe_3), 0.74 (s, 18, PMe'_3).

IR (KBr disk, cm^{-1}): 2980 (w), 2920 (m), 1448 (sh m), 1425 (s), 1405 (sh m), 1308 (m), 1300 (m), 1290 (m), 1284 (s), 1278 (sh m), 963 (vs), 858 (m), 850 (sh m), 741 (s), 735 (s), 670 (m), 340 (m), 312 (w), 300 (vw), 280 (w).

Anal. Calcd for $C_{12}H_{36}Cl_6P_4W_2$: C, 16.29; H, 4.11. Found: C, 16.39; H, 3.89.

Variable Temperature NMR Studies. ^1H NMR (toluene-d_8, δ): 21 °C, 0.95 (s, 18, PMe_3), 0.85 (s, 18, PMe'_3); 0 °C, 1.04 (s, 18, PMe_3), 0.90 (s, 18, PMe'_3); −20 °C, 1.11 (s, 18, PMe_3), 0.94 (s, 18, PMe'_3); −40 °C, 1.17 (s, 18, PMe_3), 0.98 (s, 18, PMe'_3); −60 °C, 1.22 (s, 18, PMe_3), 1.03 (br, 18, PMe'_3); −80 °C, 1.26 (s, 18, PMe_3), 1.00 (vbr, 18, PMe'_3).

$^{31}P\{^1H\}$ NMR (toluene-d_8, δ): 40 °C, −180 (br, PMe_3), −367 (vbr, PMe'_3); 22 °C, −147 (br, PMe_3), −324 (vbr, PMe'_3); 0 °C, −102 (br, PMe_3), −264 (vbr, PMe'_3); −20 °C, −70.1 (br, PMe_3), −221.0 (vbr, PMe'_3); −60 °C, −15.1 (br, PMe_3), −150.7 (br, PMe_3'); −80 °C, 0.4 (br, PMe_3), −130.5 (br, PMe'_3); −90 °C, 7.3 (br, PMe_3), −121.5 (br, PMe'_3).

Preparation of $W_2Cl_6(PEt_3)_4$. $NaW_2Cl_7(THF)_5$ (1.0 g, 1.0 mmol) was dissolved in THF (30 mL) in a 50 mL Schlenk flask equipped with

(15) Wilkins, R. G. *The Study of Kinetics and Mechanism of Reactions of Transition Metal Complexes*, Allyn and Bacon, Inc.: Boston, MA, 1974; Section 4.5.5 and references therein.

(16) Leigh, G. J.; Hills, A.; Hughes, D. L.; Prieto-Alcon, R. *J. Chem. Soc., Dalton Trans.* **1991**, 1515.

(17) $[4\text{-Me-py-H-py-4-Me}]^+[WBr_4(4\text{-Me-py})_2]^-$: Brencic, J. V.; Ceh, B.; Segedin, P. J. *J. Inorg. Nucl. Chem.* **1980**, *42*, 1409.

(18) Poli, R.; Gordon, J. C. *J. Am. Chem. Soc.* **1992**, *114*, 6723.

a Teflon-coated stir bar, and PEt_3 (1 mL, 10 mmol) was added by cannula transfer. The reaction mixture was stirred at room temperature for 12 h. The color of the solution changed from dark green to dark red. The solution was filtered and the solvent removed in vacuo. The residue was redissolved in 1:1 CH_2Cl_2–hexane (10 mL) and cooled to −10 °C for 2 days. Dark red crystals (560 mg, 0.53 mmol) were obtained in 53% yield.

^1H NMR (21 °C, toluene-d_8, δ): 1.83 (10-line m, 18, CH_2), 1.22 (q, 6, CH_2 of free PEt_3, J_{HH} = 8 Hz), 1.99 (10-line m, 36, CH_3).

$^{31}P\{^1H\}$ NMR (22 °C, toluene-d_8, δ): 26.4 (t, $^3J_{PP}$ = 40 Hz, $^1J_{PW}$ = 200 Hz (17%), $^2J_{PW}$ = 110 Hz (17%), PEt_3), −29.3 (d, $^3J_{PP}$ = 40 Hz, $^1J_{PW}$ = 210 Hz (13%), $^2J_{PW}$ = 130 Hz (13%), PEt'_3), −19.3 (s, free PEt_3), −43 (br), −173 (br, associated $W_2Cl_6(PEt_3)_4$).

$^{13}C\{^1H\}$ NMR (21 °C, toluene-d_8, δ): 19.1 (d, J_{CP} = 10 Hz, CH_2 of free PEt_3), 18.5 (s, CH_2), 17.9 (d, $^1J_{CP}$ = 10 Hz, CH_2), 15.6 (d, $^1J_{CP}$ = 27 Hz, CH_2), 9.7 (d, $^1J_{CP}$ = 10 Hz, CH_3 of free PEt_3), 8.5 (s, CH_3), 8.0, (s, CH_3), 7.6 (d, $^3J_{CP}$ = 5 Hz, CH_3), 7.1 (s, CH_3).

IR (KBr disk, cm^{-1}): 2968 (s), 2940 (s), 2910 (s), 2880 (s), 2820 (w), 2740 (w), 1455 (s), 1420 (s), 1380 (s), 1360 (m), 1040 (vs), 1020 (m), 990 (m), 980 (m), 770 (s), 750 (sh), 733 (m), 713 (s), 690 (m), 660 (w), 610 (w), 420 (w), 410 (w), 340 (m), 320 (m), 295 (s), 275 (m).

Anal. Calcd for $C_{24}H_{60}Cl_6P_4W_2$: C, 27.37; H, 5.75; Cl, 20.20. Found: C, 27.51; H, 5.84; Cl, 20.70.

Variable-Temperature NMR Studies. $^{31}P\{^1H\}$ NMR (toluene-d_8, δ, solution dissolved at room temperature): 0 °C, 27.4 (t, $^3J_{PP}$ = 40 Hz, PEt_3 of $W_2Cl_6(PEt_3)_3$), −18 (br, PEt_3 of $W_2Cl_6(PEt_3)_4$), −20.0 (s, free PEt_3), −26.4 (d, $^3J_{PP}$ = 40 Hz, PEt'_3 of $W_2Cl_6(PEt_3)_3$), −139 (br, PEt'_3 of $W_2Cl_6(PEt_3)_4$); −20 °C, 27.7 (t, $^3J_{PP}$ = 40 Hz, PEt_3 of $W_2Cl_6(PEt_3)_3$), 0.2 (br, PEt_3 of $W_2Cl_6(PEt_3)_4$), −20.6 (s, free PEt_3), −25.1 (d, $^3J_{PP}$ = 40 Hz, PEt'_3 of $W_2Cl_6(PEt_3)_3$), −119 (br, PEt'_3 of $W_2Cl_6(PEt_3)_4$); −50 °C, 27.8 (t, $^3J_{PP}$ = 40 Hz, PEt_3 of $W_2Cl_6(PEt_3)_3$), 15.2 (br, PEt_3 of $W_2Cl_6(PEt_3)_4$), −21.4 (s, free PEt_3), −23.6 (d, $^3J_{PP}$ = 40 Hz, PEt'_3 of $W_2Cl_6(PEt_3)_3$), −96 (br, PEt'_3 of $W_2Cl_6(PEt_3)_4$); −70 °C, 27.8 (t, $^3J_{PP}$ = 40 Hz, PEt_3 of $W_2Cl_6(PEt_3)_3$), 21.2 (br, t, $^3J_{PP}$ = 70 Hz, PEt_3 of $W_2Cl_6(PEt_3)_4$), −21.9 (s, free PEt_3), −22.7 (d, $^3J_{PP}$ = 40 Hz, PEt'_3 of $W_2Cl_6(PEt_3)_3$), −85 (br, PEt'_3 of $W_2Cl_6(PEt_3)_4$); −80 °C, 27.8 (t, $^3J_{PP}$ = 40 Hz, PEt_3 of $W_2Cl_6(PEt_3)_3$), 23.2 (t, $^3J_{PP}$ = 90 Hz, PEt_3 of $W_2Cl_6(PEt_3)_4$), −22.1 (s, free PEt_3), −22.3 (d, $^3J_{PP}$ = 40 Hz, PEt'_3 of $W_2Cl_6(PEt_3)_3$), −78 (br t, $^3J_{PP}$ = 90 Hz, PEt'_3 of $W_2Cl_6(PEt_3)_4$).

Preparation of $W_2Cl_6(PEt_3)_3{\cdot}CH_2Cl_2$. $W_2Cl_6(PEt_3)_4$ (0.028 g, 0.027 mmol) was dissolved in toluene (5 mL) in a 30-mL Schlenk flask equipped with a Teflon-coated stir bar and stirred for $1^1/_2$ h. The solvent was removed in vacuo, and a dynamic vacuum was applied overnight. The residue was dissolved in CH_2Cl_2 and cooled to −10 °C overnight. Red crystals (0.008 g, 0.008 mmol) were isolated in 30% yield.

Alternative Preparation of $W_2Cl_6(PEt_3)_3{\cdot}CH_2Cl_2$. $NaW_2Cl_7(THF)_5$ (0.498 g, 0.498 mmol) was dissolved in THF (20 mL) in a 50-mL Schlenk flask equipped with a Teflon-coated stir bar. PEt_3 (294 μL, 1.99 mmol) was added gradually to the solution with stirring. The color changed from green to wine-red and the solution was stirred overnight. The solution was cannula filtered and the solvent removed in vacuo. The purple oil was recrystallized from CH_2Cl_2 (8 mL) layered with Et_2O (8 mL), which was allowed to diffuse overnight at room temperature and then cooled to −10 °C for 24 h. $W_2Cl_6(PEt_3)_3{\cdot}CH_2Cl_2$ (0.125 g, 0.123 mmol) was isolated in 25% yield.

^1H NMR (23 °C, toluene-d_8, δ): 4.28 (s, 2, CH_2Cl_2), 1.84 (m, 18, CH_2), 0.97 (10-line m, 36, CH_3).

$^{31}P\{^1H\}$ NMR (20 °C, toluene-d_8, δ): 26.7 (t, $^3J_{PP}$ = 40 Hz, PEt_3), 28.6 (d, $^3J_{PP}$ = 40 Hz, PEt'_3).

IR (KBr disk, cm^{-1}): 2959 (m), 2935 (m), 2877 (m), 1669 (w), 1635 (w), 1563 (w), 1555 (1), 1455 (m), 1406 (m), 1377 (m), 1255 (m), 1036 (s), 765 (m), 735 (w), 716 (w), 693 (w), 664 (w), 615 (w), 415 (w), 319 (m), 295 (w), 249 (w).

Anal. Calcd for $C_{19}H_{47}Cl_8P_3W_2$: C, 22.38; H, 4.65. Found: C, 21.99; H, 4.48.

Preparation of $[HPEt_3]^+[W_2Cl_7(PEt_3)_2]^-$. (A) $NaW_2Cl_7(THF)_5$ (1.0 g, 1.0 mmol) was dissolved in THF (20 mL) in a 50-mL Schlenk flask equipped with a Teflon-coated stir bar, and PEt_3 (0.70 mL, 4.7 mmol) was added via syringe. In a separate 50 mL Schlenk flask, H_2O (38 μL, 2.1 mmol) was syringed into THF (10 mL). The latter was transferred into the first flask via cannula transfer. The reaction mixture was stirred at room temperature for 12 h. The solvent was then removed in vacuo. The residue was redissolved in CH_2Cl_2 (2 mL) and then layered with hexane (7 mL) and Et_2O (2 mL) in a slow diffusion flask. Crystals were grown for 2 days at 22 °C. Dark red crystals (0.723 g, 0.745 mmol) were obtained in 70% yield.

Table IX. Pertinent Data (Trials 1 and 2) Used in Obtaining Thermodynamic Parameters for Equilibrium 4

temp, °C	[L3], M	[L4], M	[L], M	K_{eq}, M	ln K_{eq}
22	0.0136	0.002 24	0.0136	0.0825	−2.49
22	0.0188	0.003 52	0.0188	0.1008	−2.30
10	0.0132	0.002 68	0.0132	0.0647	−2.74
10	0.0179	0.004 42	0.0179	0.0726	−2.62
0	0.0130	0.002 86	0.0130	0.0589	−2.83
0	0.0170	0.005 39	0.0170	0.0533	−2.93
−5	0.0130	0.002 86	0.0130	0.0589	−2.83
−5	0.0176	0.004 77	0.0176	0.0647	−2.74
−15	0.0123	0.003 49	0.0123	0.0437	−3.13
−15	0.0172	0.005 14	0.0172	0.0576	−2.85

(B) $W_2Cl_6(PEt_3)_4$ (0.097 g, 0.092 mmol) and $[HPEt_3]^+Cl^-$ (0.029 g, 0.188 mmol) were dissolved in toluene (10 mL) in a 50-mL Schlenk flask equipped with a Teflon-coated stir bar. The reaction mixture was stirred at room temperature for 12 h and then heated to 80 °C for 3 h. The solvent was reduced to approximately 1 mL and cooled to −20 °C for 2 days. Dark red crystals (0.062 g, 0.064 mmol) were obtained in 68% yield.

^1H NMR (21 °C, benzene-d_6, δ): 1.97 (dq, $P(CH_2CH_3)$), 1.6 (br, $HP(CH_2CH_3)_3$), 1.09 (dt, $P(CH_2CH_3)_3$), 0.88 (br, $HP(CH_2CH_3)_3$), 0.79 (br, $HP(CH_2CH_3)_3$).

$^{31}P\{^1H\}$ NMR (21 °C, benzene-d_6, δ): 15.78 (br, 1, $HPEt_3$), 3.26 (s, 2, PEt_3, $^1J_{WP}$ = 190 Hz (12%), $^2J_{WP}$ = 154 Hz (12%)).

IR (KBr disk, cm^{-1}): 1653 (w), 1456 (s), 1412 (s), 1381 (m), 1262 (s), 1096 (m), 1040 (vs), 978 (m), 963 (m), 870 (m), 808 (m), 758 (vs), 733 (s), 723 (vs), 702 (s), 667 (m), 623 (w).

Anal. Calcd for $C_{18}H_{36}Cl_7P_3W_2$: C, 22.26; H, 4.77; Cl, 25.55. Found: C, 23.04; H, 4.71; Cl, 24.74.

Preparation of $W_2Cl_6(P(n\text{-}Bu)_3)_4$. $NaW_2Cl_7(THF)_5$ (1.073 g, 1 mmol) was dissolved in THF (30 mL) in a 100-mL Schlenk flask equipped with a Teflon-coated stir bar. $P(n\text{-}Bu)_3$ (1.2 g, 6 mmol) was added via syringe to the reaction mixture. The solution was stirred for 24 h. The color of the solution changed from dark green to a dark red-purple. The solution was filtered using a filter stick and Celite, and the solvent of the filtrate was removed in vacuo. The residue was redissolved in CH_2Cl_2 (2 mL), layered with hexanes (15 mL), and allowed to diffuse at room temperature for 24 h. The solution was cooled at −15 °C for an additional 24 h after which a first crop of red-green crystals (580 mg, 0.417 mmol) was obtained. The solution was allowed to crystallize further at −15 °C to yield a second and subsequently a third crop of crystals (133 mg, 0.0957 mmol) (70 mg, 0.0504 mmol) respectively. The overall yield was 56.4%.

$^{31}P\{^1H\}$ NMR (21 °C, toluene-d_8, δ): 21.2 (t, $^3J_{PP}$ = 40 Hz), −31.8 (s, free $P(n\text{-}Bu)_3$), −33.6 (d, $^3J_{PP}$ = 40 Hz). The spectrum corresponds to $W_2Cl_6(P(n\text{-}Bu)_3)_3$ and free $P(n\text{-}Bu)_3$.

IR (Nujol mull, cm^{-1}): 1320 (w), 1300 (w), 1250 (w), 1230 (w), 1115 (s), 1070 (w), 1030 (w), 990 (w), 930 (m), 810 (w), 790 (m), 740 (s), 470 (w), 460 (w), 440 (w), 430 (w), 410 (w), 400 (w), 395 (w), 390 (w), 365 (m), 360 (m), 350 (m), 340 (m), 330 (m), 315 (s), 310 (s), 290 (m), 280 (m), 260 (m).

Anal. Calcd for $C_{48}H_{108}Cl_6P_4W_2$: C, 41.49; H, 7.83; P, 8.92. Found: C, 41.64; H, 7.65; P, 8.56.

Studies of the Equilibrium Involving $W_2Cl_6(PEt_3)_4$ and $W_2Cl_6(PEt_3)_3$ and Free PEt_3. General Data. The solid samples of tungsten containing compounds were weighed on a balance (±0.5 mg) in a Vacuum Atmospheres Dribox and placed in 1.0-mL volumetric flasks. Measured volumes (±20 μL) of toluene-d_8 were added under N_2 at room temperature. Samples of known concentration were placed in NMR tubes. Additions of various amounts of PEt_3 were made by use of a microliter syringe. Samples so prepared were sealed under vacuum at −178 °C and then either stored or transferred to a preequilibrated NMR probe (X °C) for study. The concentrations of the various species present in solution, $W_2Cl_6(PEt_3)_4$, $W_2Cl_6(PEt_3)_3$, and PEt_3, were estimated by integration of their ^{31}P signals. The concentration of the saturated solution of $W_2Cl_6(PEt_3)_4$ in toluene-d_8 at 22 °C is ca. 0.019 M.

Determination of K_{eq} for eq 4. Solutions of $W_2Cl_6(PEt_3)_4$ were allowed to reach equilibrium at +22, +10, 0, −5, and −15 °C. The equilibrium is approached slowly below 0 °C, and samples were stored in cold temperature baths or refrigerators set at specific temperatures. (At −30 °C, the time to reach equilibrium is greater than 5 months.)

Kinetic Approaches to Equilibrium. $W_2Cl_6(PEt_3)_4$ (20 mg, 0.019 mmol) was placed in a 1.0-mL volumetric flask and dissolved in 1.0 mL of toluene-d_8. The solution was divided into two equal portions, each was placed in an NMR tube, and a specific amount of PEt_3 was added to each. The

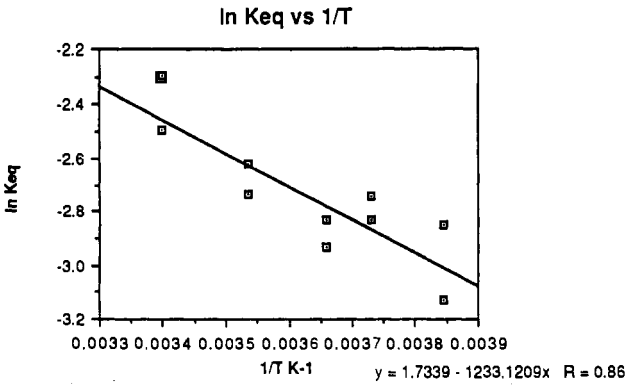

Figure 7. Plot of ln K_{eq} versus $1/T$ for the equilibrium involving $W_2Cl_6(PEt_3)_4$ and $W_2Cl_6(PEt_3)_3$ and free PEt_3.

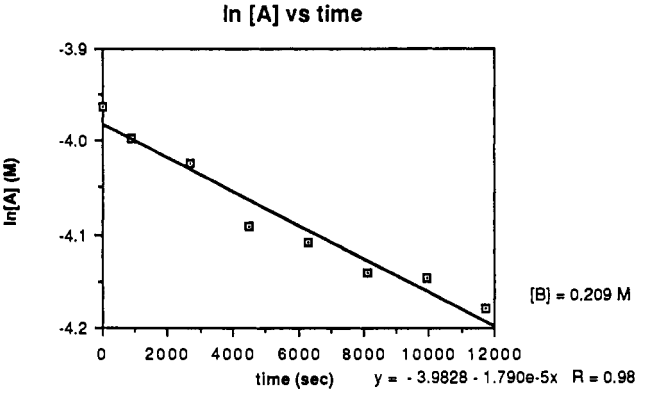

Figure 8. Plot of ln $[W_2Cl_6(PEt_3)_3]$ versus time in the formation of $W_2Cl_6(PEt_3)_4$ under pseudo-first-order conditions at 0 °C.

tubes were sealed and then heated to 60–65 °C for 3 h. At this temperature $W_2Cl_6(PEt_3)_3$ and free PEt_3 are present. The approach to equilibrium was then monitored with time at +22, +10, 0, and −10 °C. The formation of $W_2Cl_6(PEt_3)_4$ was treated according to reversible pseudo-first-order kinetics with $[PEt_3]$ in excess.

Table IX shows the pertinent data that were used in the determination of the thermodynamic parameters. Because the van't Hoff equation can be written as $\ln K_{eq} = -\Delta H°/RT + \Delta S°/R$ where R is the gas constant, a plot of ln K_{eq} versus $1/T$ was made. See Figure 7. From determination of the slope and y intercept the parameters $-\Delta H°/R$ and $\Delta S°/R$ were determined.

For the equilibrium A + B ⇄ C where A = $[W_2Cl_6(PEt_3)_3]$, B = $[PEt_3]$, and C = $[W_2Cl_6(PEt_3)_4]$, the rate can be written $d[A]/dt = k_1[A][B] + k_{-1}[C]$. When the experiment is carried out with $[B_0] \gg [A_0]$, the experiment reduces to opposing pseudo-first-order kinetics.

In our studies the equilibrium was driven to the left by heating to +60 °C and PEt_3 was present in excess. The rate of the initial reaction was

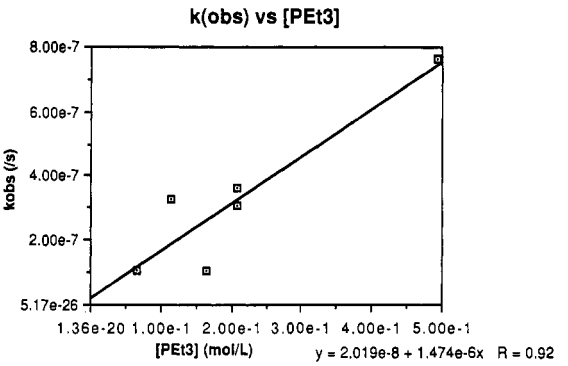

Figure 9. Plot of k_{obs} versus $[PEt_3]$ for conversion of the FSBO to ESBO $W_2Cl_6L_n$ complexes.

then determined at various temperatures with varying $[PEt_3]$. The treatment of the data then follows pseudo-first-order irreversible kinetics where a plot of ln [A] versus time is linear. This is shown in Figure 8. From the graph, the rate constant k_{obs} is given as the negative slope of the line, or for the reversible reaction $k_{obs} = k_1[B] + k_{-1}$.

Although this treatment is a simplification of the generalized reversible reaction A + B ⇄ C, it does serve to reveal whether or not there is a dependence on PEt_3 concentration. A plot of k_{obs} versus $[PEt_3]$ gave a straight line (see Figure 9) from which the rate constants k_1 and k_{-1} were obtained from the slope and y intercept, respectively.

The activation parameters were determined from a series of experiments wherein the rate constants were determined over a range of temperatures. The amount of added $[PEt_3]$ was kept constant in this series of experiments. The Arrhenius equation can be written $k = Ae^{-E_a/RT}$ where k is the rate constant, E_a is the energy of activation, R is the gas constant, T is the absolute temperature, and A is a preexponential factor. This can be rewritten in the form $\ln (K_{obs}/T) = -\Delta H^{\ddagger}(RT + \ln (k'/h) + \Delta S^{\ddagger}/R$ for which an Eyring plot of ln (k_{obs}/T) versus $1/T$ yields a straight line. The slope of the line is $\Delta H^{\ddagger}/R$ and the value of $\Delta S^{\ddagger}$ is determined from the y intercept.

X-ray Crystallographic Studies. General operating procedures and listings of programs have been provided.[19] A summary of crystal data is given in Table I, and for the sake of brevity further details have been deposited in the supplementary materials.

Acknowledgment. We thank the National Science Foundation for support and Professor Rinaldo Poli for helpful comments and criticisms.

Supplementary Material Available: Text giving details of the crystallographic determinations and tables of anisotropic thermal parameters and complete bond distances and bond angles (21 pages). Ordering information is given on any current masthead page.

(19) Chisholm, M. H.; Folting, K.; Huffman, J. C.; Kirkpatrick, C. K. *Inorg. Chem.* **1984**, *23*, 1021.